Energy landscape of a model discotic liquid crystal

Dwaipayan Chakrabarti* and David J. Wales†
University Chemical Laboratories, Lensfield Road, Cambridge CB2 1EW, United Kingdom
(Received 10 October 2007; revised manuscript received 1 February 2008; published 30 May 2008)

The potential energy surface of a model discotic liquid crystal is investigated across mesophases as a function of temperature by characterizing the local potential energy minima. The average depth of the minima sampled by the system gradually grows as orientational order increases through the discotic-nematic phase upon cooling, while it remains fairly constant in the isotropic phase for isochoric temperature variation. The high-temperature Arrhenius behavior of the single-particle orientational correlation times is found to break down at a temperature that marks the onset of exploration of deeper potential energy minima. The structural features of the minima reveal an interplay between orientational and translational order, in particular, when the parent phase is discotic-nematic. The local minima then exhibit short-range columns that tend to have local hexagonal packing. The present study and recent work on calamitic liquid crystals [D. Chakrabarti and B. Bagchi, Proc. Natl. Acad. Sci. U.S.A. **103**, 7217 (2006)] together reveal a striking similarity between thermotropic liquid crystals and supercooled liquids in the exploration of the energy landscape and the breakdown of Arrhenius behavior for relaxation times.

DOI: 10.1103/PhysRevE.77.051709 PACS number(s): 61.30.Cz, 64.70.M−, 64.70.P−

I. INTRODUCTION

Anisotropy in molecular shape plays a crucial role in the rich phase behavior that thermotropic liquid crystals display upon temperature variation [1,2]. Calamitic liquid crystals, comprised of rod-shaped molecules, are well characterized and their phase behavior and dynamics have been extensively investigated [1,2]. The discovery of discotic liquid crystals, which consist of disk-shaped molecules, is, however, more recent [3]. For discotic liquid crystals, there exist two distinct categories of mesophases: The nematic and the columnar [4]. The discotic-nematic (N_D) phase is the commonly observed nematic phase for one-component systems composed of achiral disk-shaped mesogens, where long-range orientational order exists without the involvement of any long-range translational order. The columnar phase, as the name suggests, consists of an array of columnar structures resulting from mesogens stacked on top of each other. There is long-range two-dimensional order in the plane orthogonal to the columnar axis arising from the arrangement of the columns on a regular lattice. A variety of columnar phases are known to exist, depending upon the organization of the mesogens within the columns and the symmetry of the column packing in the orthogonal plane [4]. A second kind of nematic phase, which is characterized by long-range orientational order and short-range translational order, is referred to as the nematic columnar (N_C) [5–7]. This phase occurs mainly for polymeric materials [5–7]. The translational order results from a local columnar stacking of mesogens without any symmetry in the orthogonal plane.

Discotic liquid crystals are important not only because of the fundamental interest in their exotic phase behavior, but also for their practical applications as functional materials for optoelectronic devices. The molecular architecture of discogens usually consists of a flat, rigid aromatic core with several aliphatic chains attached at its edges [7]. Many practical applications arise from the morphology of the columnar phase, which, for example, can allow one-dimensional transport of charge carriers and excitons along the columns with high carrier mobility [8]. In fact, one-dimensional charge transport in the columnar phase is of topical interest in studies of discotic liquid crystals [8–12]. The columnar phase has also enjoyed much attention in the discussion of the dynamics of discotic liquid crystals [13–17]. However, similarity in the orientational dynamics between the isotropic phase of calamitic liquid crystals near the isotropic-nematic (*I-N*) transition and supercooled molecular liquids, inferred from optical Kerr effect measurements [18], has now generated interest in the orientational relaxation in the isotropic phase of discotic liquid crystals near the phase boundaries [19–21]. In an alternative approach, the energy landscapes of calamitic liquid crystals have recently been studied using a generic model [22]. In this approach [23], the potential energy surface (PES) is partitioned into the basins of attraction, each defined as the set of points in the multidimensional configuration space for which steepest-descent pathways lead to a given local minimum of the PES. The configuration corresponding to this minimum is often called an inherent structure (IS) in the field of condensed matter [24]. A remarkable resemblance in the exploration of the PES has been found for calamitic liquid crystals [22] and glass-forming liquids [25], even though the latter systems avoid a phase transition. The energy landscape approach has, in addition, thrown light on the interplay between orientational and translational order in the calamitic mesophases [22]. Specifically, it has been found that the onset of growth in orientational order near the *I-N* phase boundary results in additional translational order in the underlying inherent structures if the parent nematic phase is sandwiched between the high-temperature isotropic phase and the low-temperature smectic phase. The latter phase is characterized by the appearance of long-range translational order in at least one dimension in addition to long-range orientational order. It is instructive to investigate whether

*dc430@cam.ac.uk
†dw34@cam.ac.uk

FIG. 1. (Color online) Snapshots of typical configurations of the mesophases observed for the discotic system studied here. From left to right: Isotropic phase, discotic-nematic phase, and columnar phase.

these results also hold for discotic liquid crystals, so as to determine their generality in the context of thermotropic liquid crystals. To this end, the present work explores the energy landscape of a model discotic system.

The literature on computer simulation studies of discotic liquid crystals is somewhat limited, especially compared to that of calamitic liquid crystals. Although atomistic simulations of realistic discogens exist [26,27], coarse-grained models of mesogens with well-defined anisotropic shapes are useful in identifying generic properties [28]. An ellipsoid of revolution offers a reasonable coarse-grained description for a discogen [28]. The simplest approach employs hard ellipsoidal bodies [29–31]. However, temperature plays no direct role here, in contrast to the thermotropic behavior observed for real mesogens [29]. Further, the formation of columnar phases by hard oblate ellipsoids of revolution is ruled out on the basis of scaling arguments [31], although their anisotropic excluded-volume interactions are sufficient to stabilize the discotic-nematic phase [29–31]. On the contrary, the Gay-Berne pair potential [32], which has been extensively used to model anisotropic interactions between soft ellipsoids [33,34], has been shown to support both the discotic-nematic and columnar phases for appropriate parameter sets with oblate ellipsoids [35]. A slightly modified version of the Gay-Berne pair potential [36], when investigated over a wider range of parameters [36–38], results in rich phase behavior for discotic liquid crystals, including a variety of columnar phases. The other anisotropic shapes that have been used in computer simulation studies of model discotic liquid crystals include cut-spheres [39], infinitely thin cylindrical segments [40], and oblate spherocylinders [41].

In the current work we have studied a system of oblate ellipsoids of revolution interacting via a modified form of the Gay-Berne (GB) pair potential, suggested by Bates and Luckhurst [36], to investigate the underlying PES. We have employed a set of parameters that we have found to support intriguing columnar phases distinct from the isotropic and discotic-nematic phases [38]. Figure 1 shows snapshots of typical configurations of the isotropic phase, the discotic-nematic phase, and a columnar phase observed for this system. In the present contribution, we focus on the exploration of the PES, especially across the I-N_D phase boundary. Our results are fairly similar to what has recently been observed for calamitic liquid crystals [22]. These studies on both calamitic and discotic liquid crystals together suggest a remarkable resemblance between thermotropic liquid crystals and glass-forming liquids [25] in the exploration of the underlying potential energy landscapes and systematic change in the high-temperature Arrhenius behavior of relaxation times.

The rest of this paper is organized as follows. Section II describes the model system studied and computational details. The results are presented in Sec. III along with discussions. Finally, we conclude with a summary of the present work and a few relevant comments.

II. MODEL AND COMPUTATIONAL DETAILS

The GB potential is a generalization of the isotropic Lennard-Jones potential that incorporates anisotropy in the attractive as well as the repulsive parts of interaction [32]. It has been extensively used as a generic model in studies of calamitic liquid crystals [33,34]. As in the original version, each ellipsoid of revolution has a single-site representation in the modified form that we employed here [36]; the ith ellipsoid of revolution is represented by the position $\mathbf{r}_i$ of its center of mass and a unit vector $\hat{\mathbf{e}}_i$ along the short axis. In this modified form the interaction between two oblate ellipsoids of revolution i and j is given by

$$U_{ij}(\mathbf{r}_{ij},\hat{\mathbf{e}}_i,\hat{\mathbf{e}}_j) = 4\epsilon(\hat{\mathbf{r}}_{ij},\hat{\mathbf{e}}_i,\hat{\mathbf{e}}_j)(\rho_{ij}^{-12} - \rho_{ij}^{-6}), \tag{1}$$

where

$$\rho_{ij} = \frac{r_{ij} - \sigma(\hat{\mathbf{r}}_{ij},\hat{\mathbf{e}}_i,\hat{\mathbf{e}}_j) + \sigma_{ff}}{\sigma_{ff}}. \tag{2}$$

Here σ_{ff} defines the thickness or equivalently, the separation between the two ellipsoids in a face-to-face configuration, r_{ij} is the distance between the centers of mass of the ellipsoids of revolution i and j, and $\hat{\mathbf{r}}_{ij}=\mathbf{r}_{ij}/r_{ij}$ is a unit vector along the intermolecular separation vector $\mathbf{r}_{ij}$. The molecular shape parameter σ and the energy parameter ϵ both depend on the unit vectors $\hat{\mathbf{e}}_i$ and $\hat{\mathbf{e}}_j$ as well as on $\hat{\mathbf{r}}_{ij}$,

$$\sigma(\hat{\mathbf{r}}_{ij},\hat{\mathbf{e}}_i,\hat{\mathbf{e}}_j) = \sigma_0\left[1 - \frac{\chi}{2}\left(\frac{(\hat{\mathbf{e}}_i\cdot\hat{\mathbf{r}}_{ij} + \hat{\mathbf{e}}_j\cdot\hat{\mathbf{r}}_{ij})^2}{1+\chi(\hat{\mathbf{e}}_i\cdot\hat{\mathbf{e}}_j)} + \frac{(\hat{\mathbf{e}}_i\cdot\hat{\mathbf{r}}_{ij} - \hat{\mathbf{e}}_j\cdot\hat{\mathbf{r}}_{ij})^2}{1-\chi(\hat{\mathbf{e}}_i\cdot\hat{\mathbf{e}}_j)}\right)\right]^{-1/2}, \tag{3}$$

with $\chi=(\kappa^2-1)/(\kappa^2+1)$ and

$$\epsilon(\hat{\mathbf{r}}_{ij},\hat{\mathbf{e}}_i,\hat{\mathbf{e}}_j) = \epsilon_0[\epsilon_1(\hat{\mathbf{e}}_i,\hat{\mathbf{e}}_j)]^{\nu}[\epsilon_2(\hat{\mathbf{r}}_{ij},\hat{\mathbf{e}}_i,\hat{\mathbf{e}}_{ij})]^{\mu}, \tag{4}$$

where the exponents μ and ν are adjustable,

$$\epsilon_1(\hat{\mathbf{e}}_i,\hat{\mathbf{e}}_j) = [1-\chi^2(\hat{\mathbf{e}}_i\cdot\hat{\mathbf{e}}_j)^2]^{-1/2} \tag{5}$$

and

$$\epsilon_2(\hat{\mathbf{r}}_{ij},\hat{\mathbf{e}}_i,\hat{\mathbf{e}}_j) = 1 - \frac{\chi'}{2}\left(\frac{(\hat{\mathbf{e}}_i\cdot\hat{\mathbf{r}}_{ij} + \hat{\mathbf{e}}_j\cdot\hat{\mathbf{r}}_{ij})^2}{1+\chi'(\hat{\mathbf{e}}_i\cdot\hat{\mathbf{e}}_j)} + \frac{(\hat{\mathbf{e}}_i\cdot\hat{\mathbf{r}}_{ij} - \hat{\mathbf{e}}_j\cdot\hat{\mathbf{r}}_{ij})^2}{1-\chi'(\hat{\mathbf{e}}_i\cdot\hat{\mathbf{e}}_j)}\right), \tag{6}$$

with $\chi'=[(\kappa')^{1/\mu}-1)]/[(\kappa')^{1/\mu}+1)]$. Here $\kappa=\sigma_{ff}/\sigma_{ee}$ is the aspect ratio of the ellipsoid of revolution with $\sigma_{ee}(=\sigma_0)$ denoting the separation between two ellipsoids of revolution

in an edge-to-edge configuration, and $\kappa' = \epsilon_{ee}/\epsilon_{ff}$, where ϵ_{ee} is the depth of the minimum of the potential for a pair of ellipsoids of revolution aligned parallel in the edge-to-edge configuration. ϵ_{ff} is the corresponding depth for the face-to-face alignment. The set of parameters that we employed in the present work was $\kappa=0.345$, $\kappa'=0.2$, $\mu=2$, and $\nu=1$. This value of κ was obtained from the parametrization for the Gay-Berne potential to mimic the interaction between two molecules of triphenylene, which is known to form the core of many discotic mesogens [35]. The value of κ' is the inverse of the one used in the most studied parametrization for the GB potential for calamitic systems [42]. We note that the same values of κ and κ' were used before in a number of computational studies [35–37]. However, we chose the exponent values to be the same as those of the most studied parametrization for the GB potential for calamitic systems [42], which also ensures that the parameters are consistent with those used in Ref. [22] as far as is practicable.

Molecular dynamics simulations were performed with a system of N oblate ellipsoids of revolution in a cubic box with periodic boundary conditions. In order to study the system size effect on the results, we considered $N=256$, $N=500$, and $N=864$. Our results were found to be qualitatively similar for these sizes. We report here the results obtained with $N=500$. All the quantities are given in reduced units, defined in terms of the Gay-Berne potential parameters ϵ_0 and σ_0, each of which is taken to be unity. Length is measured in units of σ_0, temperature in units of ϵ_0/k_B, k_B being the Boltzmann constant, and time in units of $(\sigma_0^2 m/\epsilon_0)^{1/2}$, m being the mass of the ellipsoids of revolution. We set the mass as well as the moment of inertia of each of the ellipsoids equal to unity. The intermolecular potential was truncated at a distance $r_{\mathrm{cut}}=1.6$ as in Ref. [36] and shifted for continuity. The equations of motion were integrated using the velocity-Verlet algorithm with integration time steps of $\delta t=0.0005$, 0.001, and 0.0015 (reduced units) at high, intermediate, and low temperatures, respectively [43]. Equilibration was performed by periodic rescaling of the linear and angular velocities for a period of at least 2×10^5 time steps. The system was then allowed to propagate at constant energy and density for at least another 2×10^5 time steps in order to check for equilibration. A longer equilibration time was used near the phase boundaries. Upon observation of no drift in temperature, pressure, or potential energy, data were collected in the microcanonical ensemble. The model discotic system was melted from an initial α-fcc configuration and studied along two isochors at densities of $\rho=2.6$ and $\rho=2.7$ at several temperatures. The isochors were chosen so that the system exhibits the phase sequence, isotropic, discotic-nematic, and columnar (I-N_D-C) upon cooling. However, the I-N_D phase boundary was found to be rather diffuse along the isochors, with very weak discontinuities. We therefore also investigated the system along the isobar at $P=75$ where the I-N_D transition is relatively sharp. In this case, the equilibration was performed in an NPT ensemble to adjust the system to the equilibrium density prior to data collection in the microcanonical ensemble. This adjustment should also avoid the possibility of developing cavities inside the system due to the formation of the ordered columnar structures often observed during constant volume simulations [28].

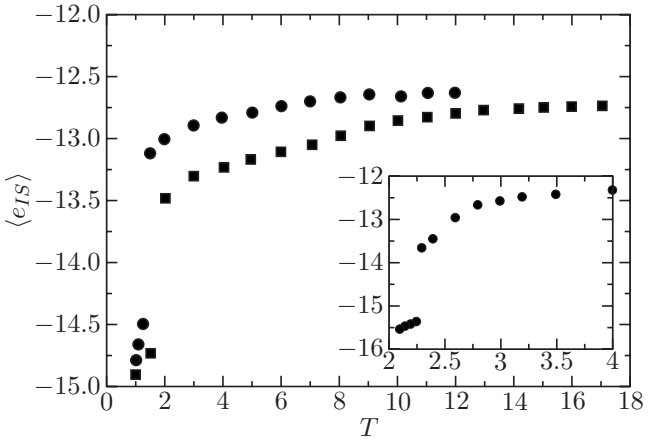

FIG. 2. Potential energy landscape explored by 500 oblate ellipsoids of revolution interacting with a modified Gay-Berne pair potential as the system passes through mesophases upon cooling. Here we show the temperature dependence of the average inherent structure energy per particle, $\langle e_{\mathrm{IS}}\rangle$, along two isochors (main frame) at densities $\rho=2.6$ (circles) and 2.7 (squares) and along an isobar (inset) at pressure $P=75$. The axis labels of the inset, which are the same as those of the main frame, are omitted for clarity.

In order to quantify the orientational order, a second-rank orientational order parameter was computed as the largest eigenvalue of the order parameter tensor,

$$S_{\alpha\beta} = \frac{1}{N}\sum_{i=1}^{N}\frac{1}{2}(3e_{i\alpha}e_{i\beta} - \delta_{\alpha\beta}), \tag{7}$$

where $\alpha,\beta=x,y,z$ are the indices referring to the space-fixed frame, $e_{i\alpha}$ is the α-component of the unit vector $\hat{\mathbf{e}}_i$, $\delta_{\alpha\beta}$ is the Kronecker symbol, and the sum goes over all N ellipsoids of revolution. At each state point, local potential energy minimization was performed by the conjugate-gradient technique for a subset of 200 statistically independent configurations unless otherwise specified. Minimization was implemented with three position coordinates and two Euler angles for each particle, the third Euler angle being redundant for ellipsoids of revolution.

III. RESULTS AND DISCUSSION

Figure 2 displays the average inherent structure energy per particle, $\langle e_{\mathrm{IS}}\rangle$, as the temperature is lowered. The corresponding evolution of the average second-rank orientational order parameter $\langle P_2\rangle$ for the prequenched configurations is shown in Fig. 3. $\langle P_2\rangle$ remains small but finite even in the isotropic phase for finite system size. The transitions between mesophases are located from the discontinuities of $\langle P_2\rangle$, which are marked by small vertical line segments. However, this discontinuity is quite small for the transition from the isotropic to the discotic-nematic phase along the isochors. In this case the onset of growth of $\langle P_2\rangle$ near the I-N_D phase boundary is marked by small vertical line segments. The phase sequence I-N_D-C appears upon cooling along both isochors and along the isobar. Further characterization of the mesophases through structural analysis is dis-

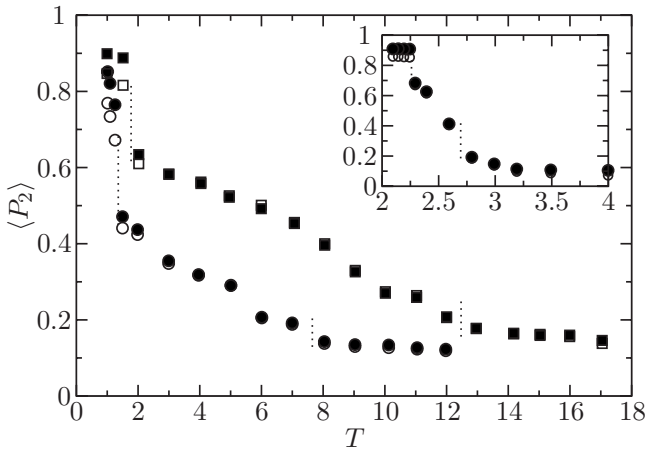

FIG. 3. Evolution of the average second-rank orientational order parameter, $\langle P_2 \rangle$, with temperature for the inherent structures (filled symbols) and for the instantaneous configurations (opaque symbols) along the isochors (main frame) at densities $\rho=2.6$ (circles) and $\rho=2.7$ (squares) and along the isobar (inset) at pressure $P=75$. The axis labels of the inset, which are the same as those of the main frame, are omitted for clarity.

cussed later. It is evident that $\langle e_{\mathrm{IS}} \rangle$ remains fairly insensitive to temperature in the isotropic phase along the isochor before it starts to fall below a certain temperature, which corresponds to the onset of growth of orientational order. Upon cooling along the isobar $\langle e_{\mathrm{IS}} \rangle$ decreases slowly, even in the isotropic phase, due to increasing density. As orientational order grows through the N_D phase, the system continues to explore deeper potential energy minima. A sharp fall in the average inherent structure energy is observed as the system crosses the N_D-C phase boundary. This observation confirms that the columnar phase is energetically much more stable. In the columnar phase, the change in the average inherent structure energy is rather small for isobaric temperature variation. Figure 3 also shows the evolution of $\langle P_2 \rangle$ for the inherent structures. It is apparent that the extent of orientational order does not change much upon quenching in the isotropic and the discotic-nematic phases. The parent columnar phase is, however, less orientationally ordered than the corresponding inherent structures.

We now consider the structural features of the various phases. In order to examine the translational structure, we computed the orientationally averaged radial distribution function $g(r)$ from the molecular dynamics trajectories prior to quenching and from the corresponding inherent structures, as shown in Figs. 4(a) and 4(b), respectively. The lack of features in $g(r)$ for the isotropic phase is suggestive of a disordered structure, even though the potential is parametrized to favor the face-to-face arrangement. However, the peak at $r \simeq 0.4$, corresponding to disks aligning in the face-to-face arrangement, tends to grow through the pretransition region and the discotic-nematic phase. The transition from the discotic-nematic to the columnar phase is marked by the emergence of the peak at $r \simeq 0.4$ as the most dominant feature of the radial distribution function. In the columnar phase, the second peak is rather broad and could be interpreted as the result of two poorly resolved peaks, one at

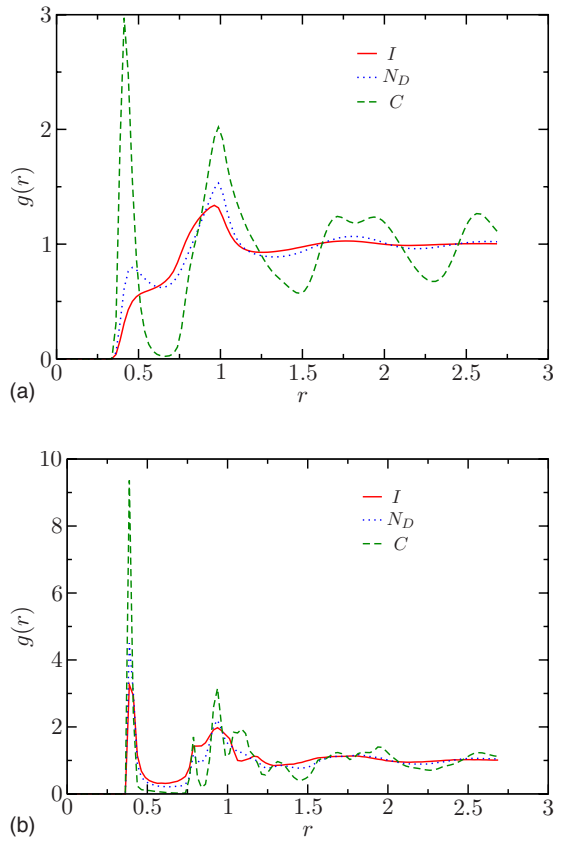

FIG. 4. (Color online) Orientationally averaged radial distribution function, $g(r)$, for a discotic system computed from (a) instantaneous configurations, and (b) the corresponding inherent structures. Here we show $g(r)$ for three different temperatures along the isobar corresponding to the isotropic phase (I), discotic-nematic phase (N_D), and columnar phase (C).

$r \simeq 0.8$ corresponding to the second-nearest columnar neighbors, and the other at $r \simeq 1$ corresponding to the edge-to-edge separation of disks in neighboring columns. Figure 4(b) suggests that quenching increases the short-range translational order as the peak at $r \simeq 0.4$ becomes the dominant one and the peak corresponding to the second-nearest neighbor in a columnar arrangement tends to be resolved. This observation can partly be attributed to the bias of the potential in favor of the face-to-face arrangement.

For a more detailed analysis of the structural features, we computed the columnar distribution function $g_c(r_\parallel)$, introduced by Veerman and Frenkel [39], which provides a measure of the extent of translational order within a column. This function is calculated by constructing a cylinder around a molecule i of radius R_c with its axis parallel to the orientational unit vector. The contribution to $g_c(r_\parallel)$ comes only from those molecules j within this cylinder for which the component of the interparticle separation vector along the cylinder axis is $r_\parallel$. The radius R_c of the cylinder was taken to be $0.5\ \sigma_{ee}$ [36,39]. The choice of the orientational unit vector, rather than the director, as the axis of the cylinder means that the columnar distribution function should be useful for the I and the N_D phases as well [36]. In Figs. 5(a) and 5(b), we show the columnar distribution function computed from the molecular dynamics trajectories prior to quenching and from

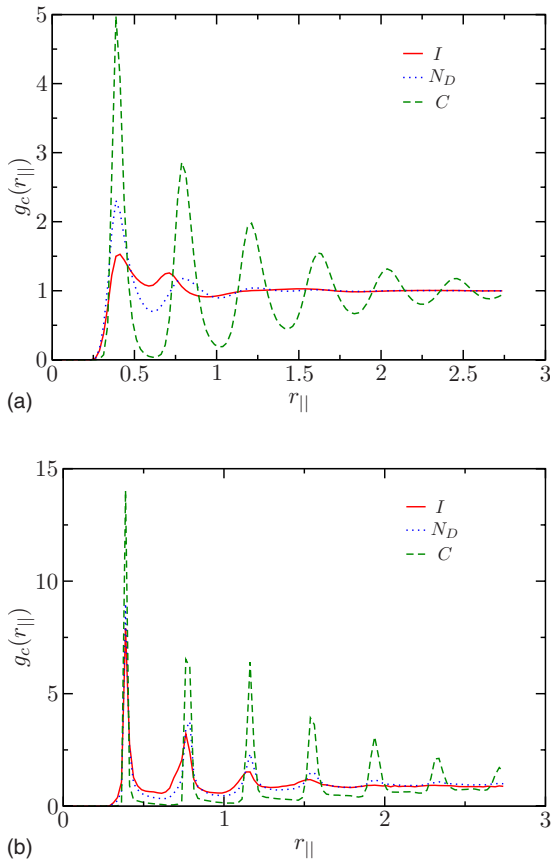

FIG. 5. (Color online) Columnar distribution function for a discotic system, $g_c(r_\parallel)$, computed from (a) instantaneous configurations, and (b) the corresponding inherent structures. Here $g_c(r_\parallel)$ is shown for three different temperatures along the isobar corresponding to the isotropic phase (I), discotic-nematic phase (N_D), and columnar phase (C).

the corresponding inherent structures, respectively. It is apparent from Fig. 5(a) that there is only weak translational order along the direction of the molecular axis in the I phase. This ordering tends to grow stronger as the system is cooled through the N_D phase. At temperatures below the N_D-C phase boundary the long-range periodic nature of $g_c(r_\parallel)$ implies column formation with periodic stacking of particles at an interparticle separation of approximately 0.4. Figure 5(b) confirms the tendency for the formation of short columns in the inherent structures of the discotic-nematic phase, in particular. The periodic structure of $g_c(r_\parallel)$ for the inherent structures becomes much stronger when the parent phase is columnar.

Figure 6 shows the perpendicular radial distribution function, $g_\perp(r_\perp)$, for the inherent structures at two representative temperatures corresponding to the N_D and C phases. For a given mesogen i, we considered the contribution to $g_\perp(r_\perp)$ from only those mesogens j for which $|\mathbf{r}_{ij}\cdot\hat{\mathbf{c}}|$ is less than or equal to 0.175, $\hat{\mathbf{c}}$ being the unit vector along the columnar axis. The choice of the columnar axis rather than the director is to allow for short columnar structures, especially for the inherent structures of the N_D phase. Each particle was assigned to a column using a distance threshold r_t=0.6 [44], and then the columnar axis was determined as the best fit

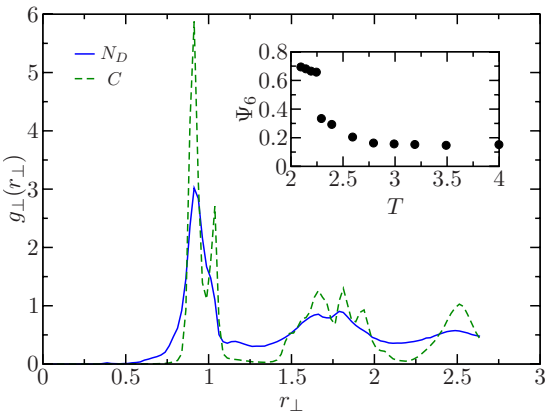

FIG. 6. (Color online) Perpendicular radial distribution function $g_\perp(r_\perp)$ for the inherent structures at two representative temperatures corresponding to the discotic-nematic phase (N_D) and columnar phase (C) along the isobar. (Inset) Hexagonal bond order parameter Ψ_6 as a function of temperature T for the inherent structures of the system along the isobar.

straight line for the centers of mass of all the particles belonging to each column. The inherent structures for the N_D phase appear to retain much of the liquidlike features in the orthogonal plane, despite the formation of the short-range columnar structures. The peak around $r_\perp$=1 splits into two across the N_D-C phase boundary, which is the signature for quasihexagonal order in the orthogonal plane [37]. The emergence of hexagonal order in the orthogonal plane is confirmed by monitoring the hexagonal bond order parameter Ψ_6 [41], which is defined as

$$\Psi_6 = \left| \left\langle \frac{1}{N}\sum_j \frac{1}{n_b^j}\sum_{\langle kl\rangle} w_{kl}\exp(6i\theta_{kl}) \right\rangle \right|. \tag{8}$$

Here n_b^j is the number of pairs of nearest neighbors of the jth particle, $\langle kl\rangle$ implies a sum over all possible pairs of neighbors, and θ_{kl} is the angle between the unit vectors along the projections of the intermolecular vectors between particle j and its neighbors k and l onto a plane perpendicular to the columnar axis. The pre-exponential factor w_{kl} was taken to be unity if the separation vectors $\mathbf{r}_{jk}$ and $\mathbf{r}_{jl}$ lie within a cylinder of radius 1.25 and thickness 0.35 centered at particle j, and zero otherwise. The inset of Fig. 6 shows the evolution of Ψ_6 with temperature for the inherent structures. We note that the hexagonal bond order parameter for the inherent structures increases through the N_D phase before it undergoes a jump across the N_D-C transition. This observation suggests a tendency for local hexagonal packing of the short-range columnar structures in the inherent structures of the N_D phase. Figure 7 shows snapshots of typical inherent structures for various parent phases of the discotic system studied here for comparison with the instantaneous configurations in Fig. 1.

Searching for a plausible correlation between the exploration of the underlying energy landscape and the dynamics of the system, we monitored the time evolution of the single-particle lth rank orientational time correlation functions (OTCF's), defined by

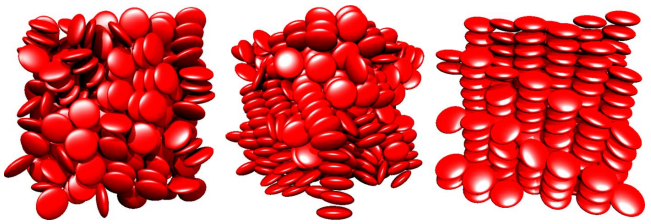

FIG. 7. (Color online) Snapshots of inherent structures corresponding to various parent phases of the discotic system. From left to right, isotropic phase, discotic-nematic phase, and columnar phase.

$$C_l^s(t) = \frac{\langle \sum_i P_l[\hat{\mathbf{e}}_i(0) \cdot \hat{\mathbf{e}}_i(t)] \rangle}{\langle \sum_i P_l[\hat{\mathbf{e}}_i(0) \cdot \hat{\mathbf{e}}_i(0)] \rangle}. \quad (9)$$

Here P_l is the lth rank Legendre polynomial and the angular brackets represent statistical averaging. We restricted ourselves to $l=1$ and 2, as $C_1^s(t)$ and $C_2^s(t)$ are directly accessible in experiments. For example, dielectric spectroscopy yields information on $C_1^s(t)$ and light scattering experiments, NMR, and electron spin resonance spectroscopies provide information on $C_2^s(t)$. The onset of the exploration of deeper potential energy minima with growing orientational order parameter is found to coincide with the emergence of a power-law relaxation regime in the time evolution of $C_2^s(t)$ near the I-N_D phase boundary (data not shown), as observed in other recent studies [19,21,45]. The slowdown of the dynamics on approaching the I-N_D transition from the isotropic side is manifested in the relaxation time $\tau_l^s(T)$. An estimate of the relaxation time was obtained by defining $\tau_l^s(T)$ as the time taken for the corresponding single-particle OTCF to decay by 90%, i.e., $C_l^s(t=\tau_l^s)=0.1$. This choice should capture the contribution from the long tail in the single-particle OTCF's, in particular, for $l=2$. Figure 8 shows the Arrhenius representation of the temperature-dependent data of the orientational relaxation times. It is evident that in the isotropic phase far from the I-N_D phase boundary, $\tau_l^s(T)$ exhibits Arrhenius behavior, i.e., $\tau_l^s(T)=\tau_{0,l}\exp[E_l/(k_BT)]$, where the activation energy E_l and the infinite temperature relaxation time $\tau_{0,l}$ are independent of temperature. The high-temperature Arrhenius behavior is found to break down near the I-N_D transition, especially for $\tau_2^s(T)$. We find that the breakdown occurs at a temperature that marks the onset of the exploration of deeper potential energy minima. Similar observations have recently been made for a calamitic system [22]. For calamitic liquid crystals, experimental results have also confirmed the breakdown of Arrhenius behavior of relaxation times in the pretransition region near the isotropic-nematic transition, which is weakly first order in nature [46].

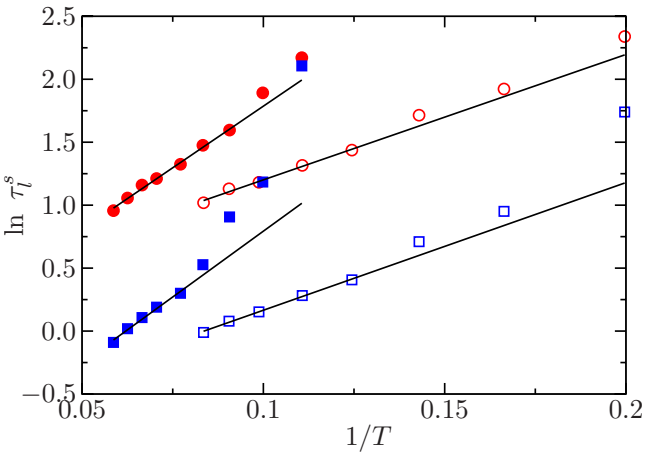

FIG. 8. (Color online) Breakdown of Arrhenius behavior in the orientational dynamics of a discotic system. The inverse temperature dependence of the single-particle orientational relaxation times, τ_l^s, is shown in the logarithmic scale: $l=1$ (circles) and $l=2$ (squares). The straight lines are Arrhenius fits for the subsets of data points, each set corresponding to a fixed density: $\rho=2.6$ (opaque symbols) and $\rho=2.7$ (filled symbols).

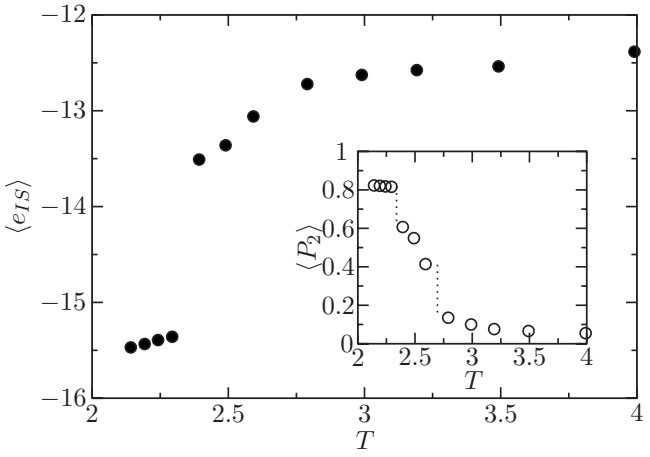

FIG. 9. Temperature dependence of the average inherent structure energy per particle, $\langle e_{IS} \rangle$, for 864 oblate ellipsoids of revolution interacting with a modified Gay-Berne pair potential as the system is cooled along an isobar at pressure $P=75$. (Inset) Evolution of the average second-rank orientational order parameter, $\langle P_2 \rangle$, with temperature for the instantaneous configurations along the same isobar.

In order to check for system size dependence, Fig. 9 shows the average inherent structure energy per particle, $\langle e_{IS} \rangle$, for $N=864$ along the isobar at pressure $P=75$ as the temperature is lowered. In this case local potential energy minimization was performed for a subset of 100 configurations at each state point. The inset shows the evolution of the average second-rank orientational order parameter $\langle P_2 \rangle$ for the prequenched configurations. It is evident that similar phase behavior is observed for this system size. The qualitative features of the temperature-dependent exploration of the potential energy minima are also found to remain the same.

IV. CONCLUSION

Let us first summarize the present work. We have explored the energy landscape of a model system of discotic liquid crystals by characterizing the inherent structures across mesophases. We find that the average depth of the potential energy minima explored by the system grows through the discotic-nematic phase as the temperature is low-

ered. In contrast, it remains fairly insensitive to temperature in the isotropic phase, in particular, along an isochor. The onset of growth in orientational order in the parent phase is found to induce translational order, arising from short-range columnar structures which tend to have local hexagonal packing. Moreover, we find that the breakdown of Arrhenius temperature dependence of the orientational relaxation times near the I-N_D phase boundary occurs at a temperature below which the system explores increasingly deeper potential energy minima.

These results are fairly similar to what has recently been observed for calamitic liquid crystals [22]. These studies on both calamitic and discotic liquid crystals together suggest a remarkable resemblance between thermotropic liquid crystals and glass-forming liquids [25] in the exploration of the underlying potential energy landscapes. The correspondence between the temperature-dependent exploration of the energy landscape and non-Arrhenius temperature dependence of the relaxation times in these soft matter systems is noteworthy. While a Gaussian distribution for the density of the potential energy minima will give rise to a temperature-dependent average inherent structure energy [47,48], it is likely that the breakdown of Arrhenius behavior is correlated with more subtle features of the underlying energy landscape [23]. As observed for calamitic systems [22], the structure of the local potential energy minima of the nematic phase is found to be different from that of the parent phase. In the present case, the structural organization of the local minima seems to be akin to that of the nematic-columnar phase, which is known to exist for some real discotic mesogens [5–7]. It is certainly of fundamental importance that the discotic-nematic phase cannot support an inherent structure of its own morphology, at least in certain cases. Such interplay between orientational and translational order suggests a role for entropy in stabilizing the nematic phase. It would be interesting to investigate the relative contributions of energy and entropy to the stability of mesophases of thermotropic liquid crystals within the energy landscape formalism.

In spite of the fundamental and practical importance of discotic liquid crystals, computational studies on these systems are somewhat limited. In this work, we restricted ourselves to a set of parameters identical to that of the most studied parametrization for the Gay-Berne model for calamitic liquid crystals in terms of the exponents μ and ν. This choice for the exponents diminishes the propensity for the formation of the columnar phase compared to the parameters used in Ref. [36]. Nevertheless, we find augmented coupling of orientational and translational order in the inherent structures. We used a value κ that compares well with a real discotic mesogen and has been used before [35–38]. The choice of κ' is reasonable to ensure the formation of the columnar phase at low temperatures [35–38]. As observed in an earlier study of calamitic systems [22], the results obtained with the present set of parameters are expected to remain qualitatively unchanged over a range of parameters for which the phase behavior is similar. It would, however, be a worthwhile exercise in the future to explore the parameter space in search of phase behavior and to study the underlying energy landscapes.

ACKNOWLEDGMENTS

We thank Professor Biman Bagchi and Professor Srikanth Sastry for stimulating discussions. One of the authors (D.C.) acknowledges support from the European Commission under the Marie Curie Program.

[1] P. G. de Gennes and J. Prost, *The Physics of Liquid Crystals* (Clarendon, Oxford, 1993).
[2] S. Chandrasekhar, *Liquid Crystals* (Cambridge University Press, Cambridge, 1992).
[3] S. Chandrasekhar, B. K. Sadashiva, and K. A. Suresh, Pramana **9**, 471 (1977).
[4] S. Chandrasekhar and G. S. Ranganath, Rep. Prog. Phys. **53**, 57 (1990).
[5] H. Ringsdorf, R. Wóstefeld, E. Zerta, M. Ebert, and J. H. Wendorff, Angew. Chem. Int. Ed. Engl. **28**, 914 (1989).
[6] P. H. J. Kouwer, W. F. Jager, W. J. Mijs, and S. J. Picken, Macromolecules **35**, 4322 (2002).
[7] S. Kumar, Chem. Soc. Rev. **35**, 83 (2006).
[8] L. Schmidt-Mende, A. Fechtenötter, K. Müllen, E. Moons, R. H. Friend, and J. D. MacKenzie, Science **293**, 1119 (2001).
[9] J. Wu, W. Pisula, and K. Müllen, Chem. Rev. **107**, 718 (2007).
[10] F. J. M. Hoeben, P. Jonkheijm, E. W. Meijer, and A. P. H. J. Schenning, Chem. Rev. **105**, 1491 (2005).
[11] J. Kirkpatrick, V. Marcon, J. Nelson, K. Kremer, and D. Andrienko, Phys. Rev. Lett. **98**, 227402 (2007).
[12] V. Lemaur, D. A. da Silva Filho, V. Coropceanu, M. Lehmann, Y. Geerts, J. Piris, M. G. Debije, A. M. van de Craats, K. Senthilkumar, L. D. A. Siebbeles, J. M. Warman, J.-L. Brédas, and J. Cornil, J. Am. Chem. Soc. **126**, 3271 (2004).
[13] S. Zamir *et al.*, J. Am. Chem. Soc. **116**, 1973 (1994).
[14] R. Y. Dong, N. Boden, R. J. Bushby, and P. S. Martin, Mol. Phys. **97**, 1165 (1999).
[15] S. V. Dvinskikh, I. Furó, H. Zimmermann, and A. Maliniak, Phys. Rev. E **65**, 050702(R) (2002).
[16] F. M. Mulder *et al.*, J. Am. Chem. Soc. **125**, 3860 (2003).
[17] J. Zhang and R. Y. Dong, Phys. Rev. E **73**, 061704 (2006).
[18] H. Cang, J. Li, V. N. Novikov, and M. D. Fayer, J. Chem. Phys. **118**, 9303 (2003).
[19] D. Chakrabarti, P. P. Jose, S. Chakrabarty, and B. Bagchi, Phys. Rev. Lett. **95**, 197801 (2005).
[20] J. Li, K. Fruchey, and M. D. Fayer, J. Chem. Phys. **125**, 194901 (2006).
[21] D. Chakrabarti, B. Jana, and B. Bagchi, Phys. Rev. E **75**, 061703 (2007).
[22] D. Chakrabarti and B. Bagchi, Proc. Natl. Acad. Sci. U.S.A. **103**, 7217 (2006).
[23] D. J. Wales, *Energy Landscapes* (Cambridge University Press, Cambridge, 2003).
[24] F. H. Stillinger and T. A. Weber, Phys. Rev. A **28**, 2408 (1983).
[25] S. Sastry, P. G. Debenedetti, and F. H. Stillinger, Nature (Lon-

don) **393**, 554 (1998).
[26] G. Cinacchi, R. Colle, and A. Tani, J. Phys. Chem. B **108**, 7969 (2004).
[27] D. Andrienko, V. Marcon, and K. Kremer, J. Chem. Phys. **125**, 124902 (2006).
[28] C. Zannoni, J. Mater. Chem. **11**, 2637 (2001).
[29] M. P. Allen, G. T. Evans, D. Frenkel, and B. M. Mulder, Adv. Chem. Phys. **86**, 1 (1993).
[30] D. Frenkel and B. M. Mulder, Mol. Phys. **55**, 1171 (1985).
[31] D. Frenkel, Mol. Phys. **60**, 1 (1987).
[32] J. G. Gay and B. J. Berne, J. Chem. Phys. **74**, 3316 (1981).
[33] M. R. Wilson, Int. Rev. Phys. Chem. **24**, 421 (2005).
[34] C. M. Care and D. J. Cleaver, Rep. Prog. Phys. **68**, 2665 (2005).
[35] A. P. J. Emerson, G. R. Luckhurst, and S. G. Whatling, Mol. Phys. **82**, 113 (1994).
[36] M. A. Bates and G. R. Luckhurst, J. Chem. Phys. **104**, 6696 (1996).
[37] D. Caprion, L. Bellier-Castella, and J.-P. Ryckaert, Phys. Rev. E **67**, 041703 (2003).
[38] D. Chakrabarti and D. J. Wales, Phys. Rev. Lett. **100**, 127801 (2008).
[39] J. A. C. Veerman and D. Frenkel, Phys. Rev. A **45**, 5632 (1992).
[40] M. A. Bates and D. Frenkel, Phys. Rev. E **57**, 4824 (1998).
[41] H. Zewdie, Phys. Rev. E **57**, 1793 (1998).
[42] E. de Miguel and C. Vega, J. Chem. Phys. **117**, 6313 (2002).
[43] J. M. Ilnytskyi and M. R. Wilson, Comput. Phys. Commun. **148**, 43 (2002).
[44] R. Berardi, M. Cecchini, and C. Zannoni, J. Chem. Phys. **119**, 9933 (2003).
[45] D. Chakrabarti and B. Bagchi, J. Phys. Chem. B **111**, 11646 (2007).
[46] A. Drozd-Rzoska, S. Rzoska, S. Pawlus, and J. Ziolo, Phys. Rev. E **72**, 031501 (2005).
[47] S. Büchner and A. Heuer, Phys. Rev. E **60**, 6507 (1999).
[48] D. J. Wales and J. P. K. Doye, Phys. Rev. B **63**, 214204 (2001).